

## **Polythiophene Coated Cellulosic Fibers from Banana Stem for Improved Electrical, Mechanical, Thermal and Dielectric Properties of Polypropylene Composites**

**J. Thekkedath<sup>1</sup>, P. K. Bipinbal<sup>1</sup>, T. Thomas<sup>2</sup>, S. K. Narayanankutty<sup>1\*</sup>**

<sup>1</sup>Department of Polymer Science & Rubber Technology, Cochin University of Science & Technology, Kochi, Kerala, India

<sup>2</sup>Department of Chemistry, St. Peter's College, Kolenchery, Ernakulam, Kerala, India

Received 5 December 2019, accepted in final revised form 18 March 2020

### **Abstract**

Incorporating conducting polymer coated fibers in a nonconducting base polymer has proven to be an effective method for the preparation of conducting composites. In the present work, banana fibers, cellulosic microfibers from waste biomass, were used for the coating of conducting polymer through in situ polymerization of thiophene on the fiber surface. The polythiophene (PTH) coated fibers were used as the conducting elements in a general-purpose thermoplastic, polypropylene (PP). The prepared composites were examined for electrical, thermal, mechanical, dynamic mechanical and dielectric properties. Formation of a continuous conducting network of PTH coated fibers in the polymer matrix imparted 6 fold increase in conductivity, 22 % improvement in tensile strength and 47% improvement in tensile modulus. Thermal degradation temperature of polypropylene was improved up to 26 °C. An exceptional improvement of more than 3 orders of magnitude in dielectric constant could be achieved for the composites making them suitable for capacitor applications.

*Keywords:* polythiophene, polypropylene, conducting cellulose fiber, composites, dielectric properties

© 2020 JSR Publications. ISSN: 2070-0237 (Print); 2070-0245 (Online). All rights reserved.  
doi: <http://dx.doi.org/10.3329/jsr.v12i4.45774>

J. Sci. Res. **12** (4), 687-699 (2020)

### **1. Introduction**

Discovery of polymers with intrinsic electrical conduction has been a major milestone in polymer engineering opening up a wide range of potential applications. Polythiophene (PTH) is one of the important conducting polymers studied extensively on account of its good environmental stability, unique redox electrical behavior, stability in doped or neutral states, ease of synthesis and possibility of applications in many fields [1,2]. A major limitation for wider application of conducting polymers in general and polythiophene in particular is low processability resulting from insolubility and

---

\*Corresponding author: [sncusat@gmail.com](mailto:sncusat@gmail.com)

infusibility. To overcome this problem composites of polythiophene have been made by dispersing it in easily processable insulating polymers [3]. Composites thus prepared combine the electrical properties of polythiophene and processability, mouldability and flexibility and other desirable mechanical properties of the base polymer.

Conductivity of a composite prepared by combining conducting elements and insulating matrix is attributed to the formation of a network of the conducting elements within the matrix. The efficiency of conduction depends on the integrity of the formed network apart from the conductivity of the constituting elements. If the conducting elements are in the form of fibers, formation of a continuous network is possible even at low volume fraction of the conducting component. To this end, either conducting polymers can be made in the form of fibers [4,5] or a non-conducting fiber can be coated with a conducting polymer [6-8].

Cellulose, the most abundant and renewable biopolymer on earth, is noted for its biodegradability and high strength to weight ratio. It is mostly found in the primary cell wall of plants, where cellulose molecules are arranged in arrays to form nanofibrils, which in turn associate to form fibers in micro dimensions. Cellulosic fibers have been successfully utilized as reinforcing members in general purpose polymers [9-13]. There have been reports of cellulosic fibers coated with conducting polymers. Polyaniline and silver nanoparticles were used to coat cellulosic fibers in the work by Stejskal *et al.* [14]. They found that increasing the aspect ratio of the fibers decreased the percolation threshold. Vapour phase polymerisation of pyrrole was performed on cellulose-based textiles [15]. Souza *et al.* modified curauá fibers with polyaniline nanoparticles and probed the feasibility to use it as a pressure sensing material. Dip coating of microcrystalline cellulose was carried out using PEDOT: PSS and it was found that PEDOT was the preferential adsorbent compared to PSS [16]. Coir micro and nanofibers were coated with polyaniline and incorporated in natural rubber to prepare conducting composites [17]. Razak *et al.* [18] prepared composites of epoxy resin and polyaniline coated cellulosic fibers from kenafbast. Polyvinyl alcohol was used to prepare composites of polyaniline coated cellulosic fiber composites with low percolation threshold [19].

In the present work cellulosic fibers from banana stem, an agricultural waste found aplenty in the southern states of India, is used. A coating of PTH on the fiber was formed by in situ polymerization. The coated fibers were then incorporated into polypropylene in an internal mixer and the composites were prepared by compression molding in a hydraulic press. The composites were evaluated for thermal, mechanical and electrical properties.

## **2. Materials and Methods**

### **2.1. Materials**

Polypropylene was purchased from Alpha Chemicals, India. Banana stem fibers were collected locally and were chopped to short fibers of 10 mm length. Thiophene, ferric chloride, dichloromethane and acetonitrile were supplied by E-Merck Mumbai, India.

## 2.2. Preparation of PTH coated fiber

Banana fibers were washed with distilled water and dried. 16 g of banana fibers were soaked in dichloromethane solution of thiophene (16 mL dissolved in 600 mL) for 30 min. 130 g of ferric chloride was dissolved in 300 mL acetonitrile and added drop wise to the banana fiber/thiophene mixture. The reaction mixture was stirred for 2 h after which 10 mL of hydrogen peroxide (30 %) was added slowly to convert ferrous ions formed to ferric ions. The stirring was continued for 2 more h. The resultant mixture was washed with acetonitrile and ether until the washings were colourless. Washed polythiophene coated fibers were dried at 70 °C and incorporated into polypropylene in the required amount.

## 2.3. Preparation of PTH coated fiber/PP composites

Mixing was done in a Brabender plastograph at 145 °C. When PP was softened due to temperature and shear, PTH coated fiber was added slowly and the mixing was continued for another 5 min. The mix was then removed and pressed between aluminium platens. The pressed sheets were granulated and used for compression moulding. Moulding was done in a hydraulic press at a temperature of 150 °C under 200 MPa pressure.

Table 1. Formulation of PTH coated fiber/PP composites.

Contents	phr				
PP	100	100	100	100	100
PTH coated fiber	0	10	20	30	40

## 2.4. Characterization methods

Infrared spectrum was recorded on a Bruker FTIR spectrophotometer model Tensor 27 (spectral range of 4000 to 600  $\text{cm}^{-1}$  with standard KBr beam splitter) in attenuated total reflectance (ATR) mode. Scanning electron microscope studies were carried out using SEM model 6390LA JEOL instrument. Samples were sputter coated with gold for 25 s. Mechanical properties were measured using Shimadzu Universal Testing Machine Model AG-I 10 kN according to ASTM D638. Thermogravimetric analysis was carried out on TA Instruments TGA Q50 at a heating rate of 20 °C/min under nitrogen atmosphere. DC electrical conductivity of PTH and PTH/PP composites were measured by a two-probe method using a Keithley 2400 source-measure unit. Dielectric measurements were carried out at frequencies ranging from 40 to 8 kHz using an impedance analyzer, Agilent E 4980 A Precision LCR Meter.

### 3. Results and Discussion

#### 3.1. Fourier transform infrared spectroscopy

FTIR spectra of PTH, cellulosic fiber and PTH coated fiber are shown in Fig. 1. Characteristic bands of PTH are seen in the spectrum of PCF confirming successful in situ polymerization of thiophene on fiber surface. The band at  $643\text{ cm}^{-1}$  corresponds to C-S-C stretching in thiophene ring [20]. Vibration bands observed at  $1155\text{ cm}^{-1}$  and  $1033\text{ cm}^{-1}$  are due to C-H bending and C-H in plane deformation [20]. The characteristic band of PTH indicating 2,5-disubstitution seen at  $787\text{ cm}^{-1}$  [20-22].

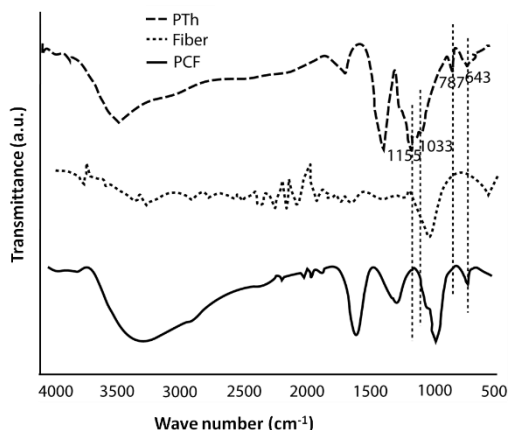


Fig. 1. FTIR spectra of PTH, fiber and PTH coated fiber.

#### 3.2. Morphology

SEM images of uncoated and PTH coated banana fibers in different magnifications are shown in Figs. 2 and 3, respectively. The banana stem fibers are found to be an association of large number of microfibrils each having a width of 10 to 20  $\mu\text{m}$ . The magnified versions of the uncoated fibers show striations and ridges on the microfibrils which will be helpful in anchoring the in situ formed PTH particles on the fiber surface. After the in situ coating of PTH, the fiber bundles are seen separated into individual fibers (Fig. 3). During in situ coating the fiber bundle remains soaked in dichloromethane for 30 min, which swells the fibers and seeps into the inter-fibrillar space causing them to separate. Subsequent stirring during polymerization ensures the complete separation of all the microfibrils from each other which get coated with PTH. A more or less uniform coating of PTH can be seen throughout the surface of the microfibrils.

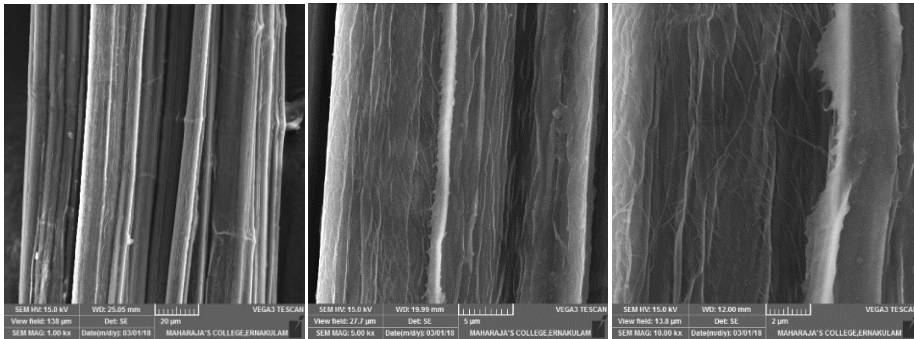


Fig. 2. SEM images of uncoated banana fibers at different magnifications.

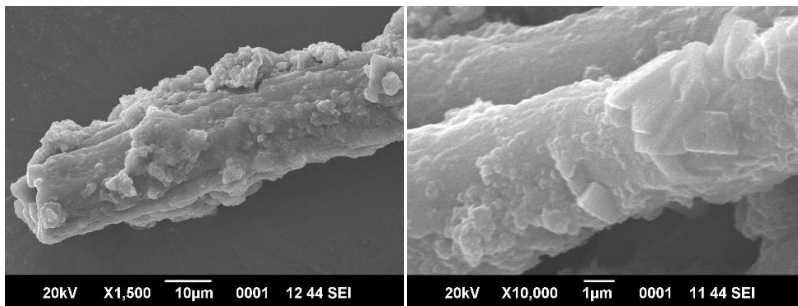


Fig. 3. SEM images of banana fiber coated with PTH at different magnifications.

SEM images of the fracture surface of PTH coated fiber/PP composites with 40 phr fiber loading are given in Fig. 4. PTH coated fibers are seen emedded in the polypropylene matrix. In the fracure surface longitudinal arrays of coated fibers are seen to be intersecting at different angles. The composite under examination, on account of its high fiber content (40 phr), shows poor dispersion resulting in fiber agglomeration in the matrix. Closer examination of another area on the fractured surface shows elongated matrix and fibrils. The yielding of matrix under stress leads to the formation of matrix fibrils. Similar morphology has been reported by Premalal *et al.* [23] and Pang *et al.* [24] in their studies of PP based fiber composites.

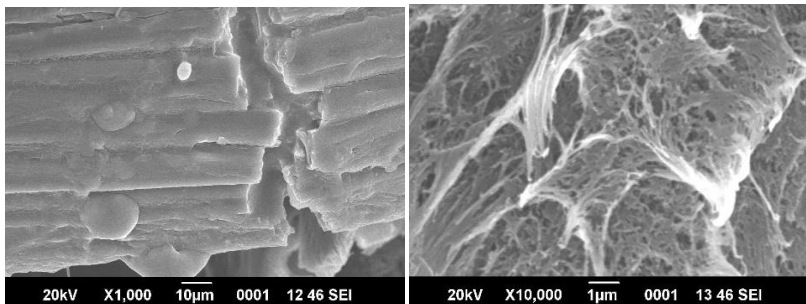


Fig. 4. SEM images of PTH coated fiber/PP composite (40 phr) at different magnifications.

### 3.3. Thermal studies

Thermogravimetric analysis of banana fiber, PTH coated banana fiber, pure PP and PTH coated fiber/PP composites is depicted in Figs. 5 and 6. Thermogravimetric curves are plotted in Fig. 5 and derivative thermogravimetric curves in Fig. 6. The weight loss of both fiber and PTH coated fiber up to about 130 °C accounts for the moisture content in the fiber and absorbed moisture in the PTH. The peak beyond 130 °C and extending up to 210 °C in the case of PTH coated fiber may be attributed to the loss of moisture entrapped below the PTH layer on the fiber surface. The escape of this water during drying in an oven is prevented by the PTH coating. The same coating prevents the removal of this entrapped water at lower temperatures at which loss of adsorbed water on the surface occurs during thermogravimetric analysis. This water is removed at higher temperature which is expressed as a delayed loss in weight. A small peak beyond 210 °C in the DTG curve of coated fiber may be from the loss of hemicellulose content of the banana fiber. The peak coincides with the corresponding peak in the DTG curve of the banana fiber which overlaps with the main peak of cellulose degradation. Interestingly degradation rate of cellulose in the PTH coated banana fiber is found to be greatly reduced which can be credited to the coating of PTH on the fiber surface and lower degradation rate of PTH compared to the cellulosic fiber. The small peaks appearing in the range 450 - 550 °C and 550 - 650 °C may be attributed to the degradation of components from lignin and main chain degradation of PTH respectively.

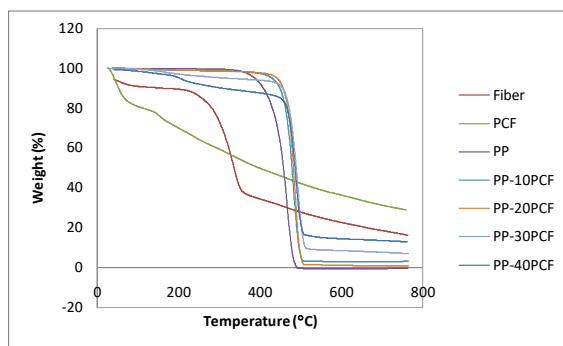


Fig. 5. Thermogravimetric curves of banana fiber, PTH coated banana fiber (PCF), PP and PCF/PP composites.

The PTH coated fiber/PP composites show a weight loss which can be due to the loss of moisture from the samples. Banana fibers contain a moisture content of more than 10 %. The moisture that remains entrapped within the fiber even after the drying operation in the oven, due to coating of PTH on the fiber surface, is removed during thermogravimetric analysis, albeit at higher temperature. However, PTH coated fiber filled samples show higher thermal stability compared to pure PP sample (Fig. 5). This can be attributed to the higher thermal stability of PTH. As evident from the degradation profile of PTH coated fiber, the coating of PTH greatly reduces the degradation rate of cellulosic fiber. A randomly oriented network of thermally resistant PTH coated

fibers formed inside the PP matrix is responsible for the delayed degradation of the composites. Pure PP samples degrade completely with almost no residue. Coated fiber composites show residues corresponding to the content of PTH in the samples. This points to the formation of a char by the degradation of PTH which act as a heat barrier and improves the thermal stability of the composites.

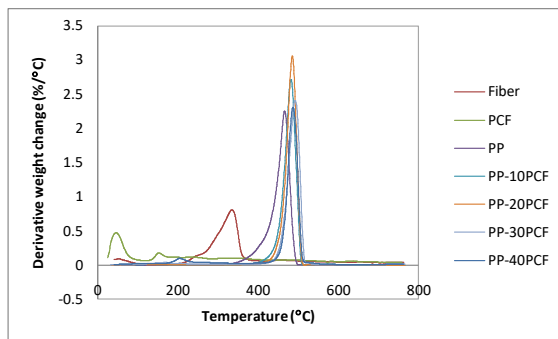


Fig. 6. Derivative thermogravimetric curves of banana fiber and PTH coated banana fiber (PCF), PP and PCF/PP composites.

### 3.4. Mechanical properties

Variation of tensile strength of the composites with respect to the PTH coated fiber content is shown in Fig. 7. 10 phr of PTH coated fiber significantly improves the tensile strength of PP. This can be attributed to the formation of a network of PTH coated fiber inside the matrix by the polar-polar association. At higher loadings tensile strength of the composites decreases. This may due to the agglomeration of fibers inside the matrix which impairs efficient stress transfer between the matrix and the fiber. This leads to stress concentration in the composites resulting in premature failure. However, the values are higher than that of samples without fibers. At 40 phr fiber loading the composite retains the tensile strength of the pristine matrix.

The effect of PTH coated fiber on tensile modulus is depicted in Fig. 8. The tensile modulus increases with the fiber content almost in a linear fashion. The coated fibers dispersed in the matrix impart higher rigidity to the matrix by forming a network of interconnected randomly oriented fibers. This fiber skeleton offers more resistance to deformation which may be credited to the strong interactive association between the member fibers. This may compensate for the poor interaction between the fiber and the matrix. As the fiber content increases the network becomes more rigid, which is reflected as increased modulus of the composites.

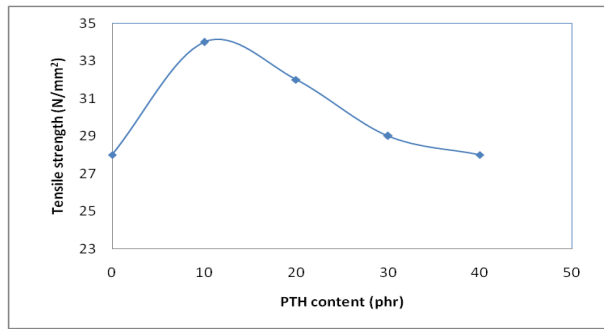


Fig. 7. Variation of tensile strength with PTH coated fiber content in PTH coated fiber/PP composites.

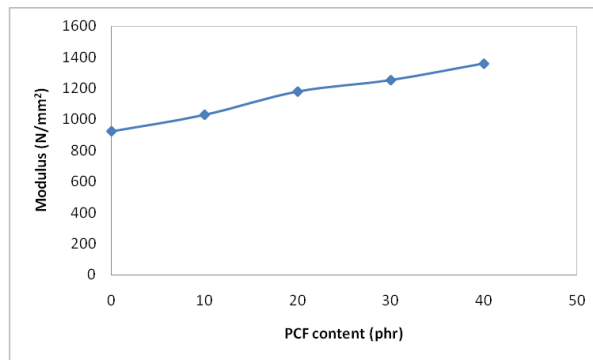


Fig. 8. Variation of tensile modulus with PTH coated fiber content in PTH coated fiber/PP composites

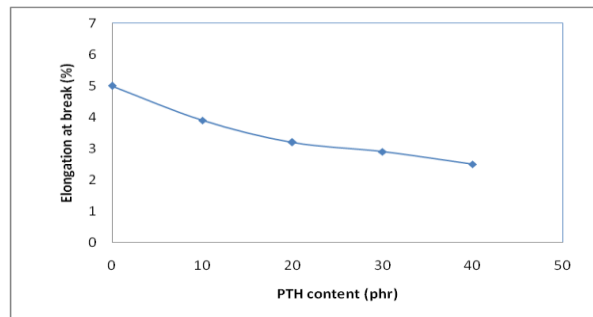


Fig. 9. Variation of elongation at break with PTH coated fiber content in PTH coated fiber/PP composites.

Influence of fiber content on elongation at break of the PTH coated fiber/PP composites is illustrated in Fig. 9. With increasing fiber content, elongation at break is reduced as the fiber immobilises PP chains. Increased restriction to the mobility of PP molecules imposed by the network of fibers results in lower ultimate elongation. Agglomeration of fibers at higher loadings results in stress concentration leading to premature failure of the composites.



### 3.5. Conductivity studies

Effect of PTH coated fiber content on DC conductivity of PTH coated fiber/PP composites is given in Fig. 10. Conductivity increases with PTH coated fiber content and the increase becomes significant beyond a loading of 20 phr. As the non-conducting cellulosic fiber excludes the volume required to be filled up with the conducting PTH, the PTH coating on the surface of the fibers together with the free PTH in the matrix are expected to bring about higher conductivity. But the conductivity improvement is not as high as expected. This may be due to the presence of moisture in the coated fibers which amounts to about 10 % of the fiber weight as evident from thermogravimetric analysis. Water molecules can react with PTH coating on the fiber surface, causing incorporation of carbonyl groups in the PTH molecules. These carbonyl groups break the conjugation in PTH molecules rendering the polymer nonconductive [25]. Apart from this,  $\text{FeCl}_3$  dopant present in the PTH layer may migrate to the fiber surface and get dissolved in the moisture entrapped in coated fibers of the composites. Migration and deposition of simple molecules on to the fiber surface has been reported earlier [26,27]. The dissolved  $\text{FeCl}_3$  may get absorbed further into the interior of the fibers making it unavailable for the doping purpose. These factors may reduce the conductivity of the coating and in turn the conductivity of the composites.

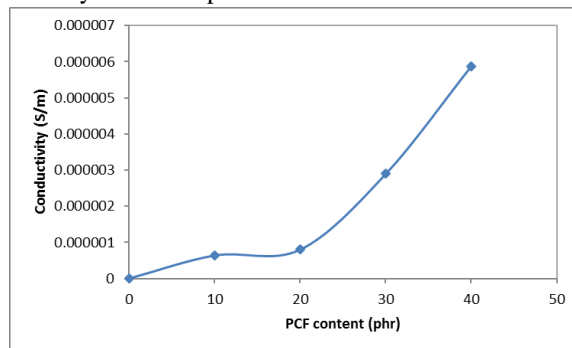


Fig. 10. Variation of DC conductivity with PTH coated fiber content of PTH coated fiber/PP composites.

### 3.6. Dynamic mechanical properties

Variation of storage modulus of PCF/PP composites with frequency in dynamic mechanical analysis conducted in the frequency sweep mode is shown in Fig. 11. Storage modulus increases with frequency, which is more pronounced at higher PCF content composites at lower frequencies. Coated fibers distributed in the PP matrix associate themselves to form a network imparting rigidity to the matrix. In dynamic mechanical analysis lower frequency is equivalent to higher temperature where molecular mobility is higher decreasing the modulus of the samples. At higher temperatures the matrix becomes flexible and would no longer be able to support the integrity of the coated fiber network. So, under the action of the dynamic force the network collapses causing a reduction in the modulus of the composites. At higher fiber content fiber network is more extensive and the effect of its collapse is greater leading to a higher decrease in modulus.

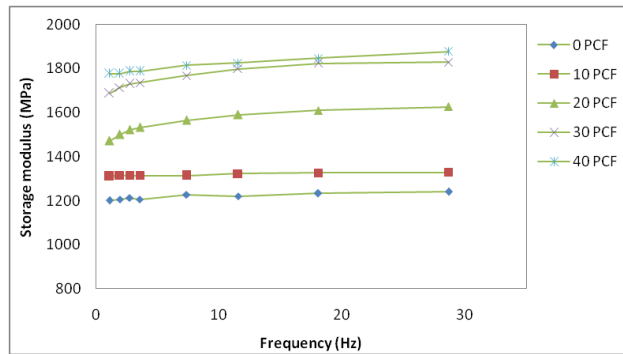


Fig. 11. Variation of storage modulus of PCF/PP composites with frequency.

Effect of frequency and coated fiber content on loss modulus of the composites is depicted in Fig. 12. Loss modulus, a measure of energy dissipated, shows an inverse trend as that of storage modulus giving a decrease with increase in frequency. This is more pronounced at lower frequencies. Low frequency or higher temperature gives rise to molecular mobility and collapse of the fiber network rendering the composites with more viscous nature. So, more energy is dissipated at lower frequencies giving higher loss modulus. As the frequency increases molecular mobility is restricted reducing the energy dissipation and hence loss modulus. The reduction in loss modulus is higher in composites with higher fiber content where the collapse of fiber network at higher temperatures results in higher loss modulus. With increase in fiber content loss modulus increases. Being polar, PTH and fiber exhibit an inherent incompatibility with the nonpolar PP matrix giving rise to poor stress transfer and hence energy dissipation at respective interfaces. At higher coated fiber content interfacial area also becomes higher, inducing higher energy dissipation and loss modulus.

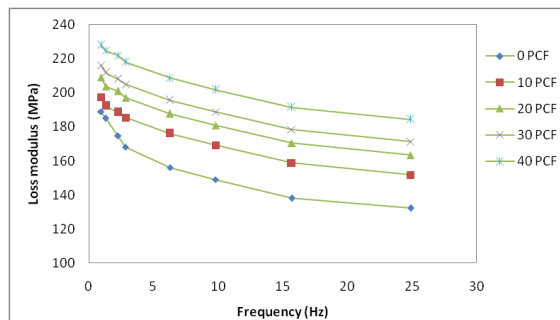


Fig. 12. Variation of loss modulus of PCF/PP composites with frequency.

Variation of  $\tan \delta$  with frequency and fiber content is shown in Fig. 13.  $\tan \delta$ , ratio of loss modulus to storage modulus, emulates the behaviour of loss modulus with respect to frequency. But with increase in fiber content  $\tan \delta$  decreases. This shows that increase in

storage modulus with fiber content is higher compared to the increase in loss modulus. In other words, restriction imposed on molecular mobility by the fiber network is higher compared to the energy lost at the interfaces.

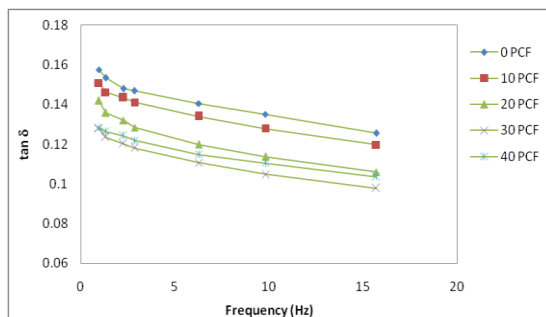


Fig.13. Variation of  $\tan \delta$  of PCF/PP composites with frequency.

### 3.7. Dielectric properties

Dielectric properties of pure PP and PTH coated fiber/PP composites were analysed with respect to frequency and fiber content. Variation of dielectric constant is given in Fig. 14 and that of dielectric loss in Fig. 15. Pure PP shows very low dielectric constant and dielectric loss which is credited to the absence of any dipoles or heterogeneity in conduction. On addition of PTH coated fiber the composites show large increase in dielectric constant. This can be attributed to the introduction of dipolar and interfacial polarization in the composites by the incorporation of PTH coated fibers. Dipoles on PTH molecules from the dopant,  $\text{FeCl}_3$ , and inherent dipoles in the cellulosic fiber are responsible for dipolar polarization by orienting themselves in the alternating electric field. Interfacial polarization arises from the difference in conductivity of individual components in the composites and ensuing charge accumulation at the interface. PTH-fiber, PTH-matrix and fiber-matrix interfaces are possible sites for charge accumulation and resultant polarization. With increase in fiber content dipolar and interfacial polarizations also increase leading to high dielectric constant. With increase in frequency dielectric constant of the composites decreases which is significant at lower frequencies. The decrease gradually reduces with frequency and levels off at higher frequencies. As the frequency increases dipoles fail to follow the alternating electric field and lag behind. This results in gradual decrease in dipolar polarization and dielectric constant.

Variation of dielectric loss is similar to that of dielectric constant in respect of frequency and coated fiber content. Dipoles present in the composites align themselves with the alternating electric field by changing orientation in every cycle. The resultant friction between the dipoles and the surrounding molecules cause heat generation which is expressed as dielectric loss in the material. With higher fiber content, number of dipoles also increases, intensifying the heat generation and hence escalating dielectric loss.

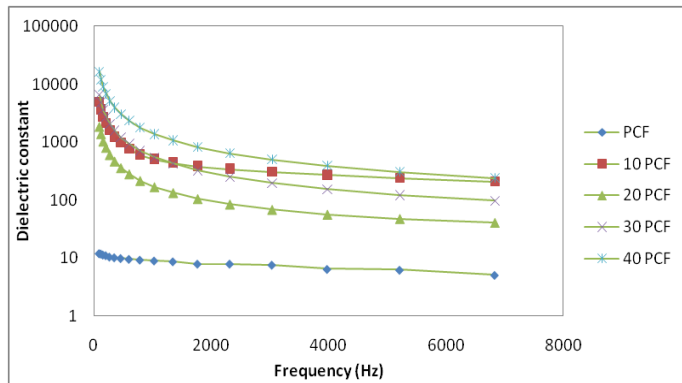


Fig. 14. Variation of dielectric constant of PTH coated fiber/PP composites with frequency.

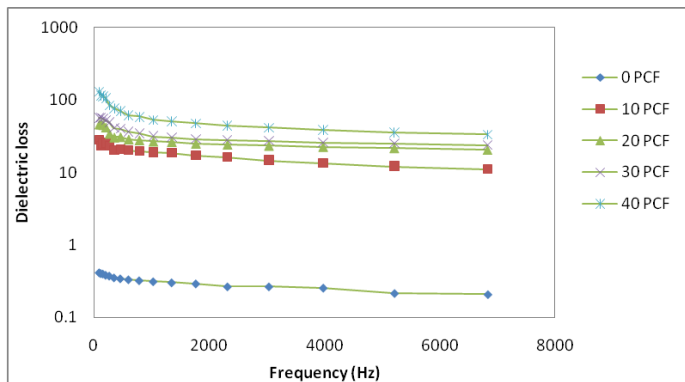


Fig. 15. Variation of dielectric loss of PTH coated fiber/PP composites with frequency.

#### 4. Conclusion

Polythiophene was coated onto cellulosic fibers from banana stem through in situ oxidative polymerization. FTIR, SEM and thermogravimetric characterization confirm successful adherence of PTH on fiber. Conducting composites can be prepared by incorporating PTH coated fiber into polypropylene matrix through melt mixing in an internal mixer. A continuous random network of coated fibers is formed within the PP matrix which is able to improve tensile strength of the composite by 22 % at low fiber content. Tensile modulus is improved (47 %) by the incorporation of coated fibers while elongation at break is reduced. Thermal analysis shows moisture entrapment in coated fibers. Coated fibers are effective in delaying the thermal degradation of the composites up to 26 °C. Moisture in the cellulosic fibers reduces the conductivity of the composites. Even then PTH coated fibers are able to impart 600 % increase in conductivity. Very high dielectric constant of the order of  $10^4$  could be achieved through incorporation of PTH coated fibers in PP which can be utilized in capacitor applications.

## References

1. S. Yigit, J. Hacaloglu, U. Akbulut, and L. Toppare, *Synth. Met.* **79**, 11 (1996).  
[https://doi.org/10.1016/0379-6779\(96\)80123-8](https://doi.org/10.1016/0379-6779(96)80123-8)
2. R. S. Bobade, *J. Polym. Eng.* **31**, 209 (2011). <https://doi.org/10.1515/polvorg.2011.044>
3. J. Njuguna and K. Pielichowski, *J. Mater. Sci.* **39**, 4081 (2004).  
<https://doi.org/10.1023/B:JMASC.0000033387.51728.de>
4. J. Huang, *Pure Appl. Chem.* **78**, 15 (2006). <https://doi.org/10.1351/pac200678010015>
5. A. Luzio, E. Canesi, C. Bertarelli, and M. Caironi, *Materials* **7**, 906 (2014).  
<https://doi.org/10.3390/ma7020906>
6. R. V. Gregory, W. C. Kimbrell, and H. H. Kuhn, *Synth. Met.* **28**, 823 (1989).  
[https://doi.org/10.1016/0379-6779\(89\)90610-3](https://doi.org/10.1016/0379-6779(89)90610-3)
7. C. Merlini, B. S. Rosa, D. Muller, L. G. Ecco, S. D. Ramoa, and H. M. Barra, *Polym. Test.* **31**, 971 (2012). <https://doi.org/10.1016/j.polymertesting.2012.07.003>
8. N. Muthukumar and G. Thilagavathi, *Ind. J. Chem. Technol.* **19**, 434 (2012).
9. R. Goyena and A. Fallis, *J. Chem. Inf. Model.* **53**, 1689 (2019).
10. M. Islam, A. Sharif, M. Hussain, and I. Hassan, *Bangl. J. Sci. Ind. Res.* **54**, 21 (2019).  
<https://doi.org/10.3329/bjsir.v54i1.40727>
11. K. Begum, M. A. Islam, and M. M. Huque, *J. Sci. Res.* **7**, 97 (2015).  
<https://doi.org/10.3329/jsr.v7i3.23075>
12. K. Begum and M. A. Islam, *J. Sci. Res.* **11**, 89 (2019). <https://doi.org/10.3329/jsr.v11i1.36450>
13. M. R. Hossain, F. Hossain, and M. A. Islam, *J. Sci. Res.* **6**, 431 (2014).  
<https://doi.org/10.3329/jsr.v6i3.15811>
14. J. Stejskal, M. Trchová, J. Kovářová, J. Prokeš, and M. Omastová, *Chem. Pap.* **62**, (2008).  
<https://doi.org/10.2478/s11696-008-0009-z>
15. L. Dall'Acqua, C. Tonin, A. Varesano, M. Canetti, W. Porzio, and M. Catellani, *Synth. Met.* **156**, 379 (2006).
16. E. Montibon, L. Järnström, and M. Lestelius, *Cellulose* **16**, 807 (2009).  
<https://doi.org/10.1007/s10570-009-9303-3>
17. P. K. Bipinbal, Preparation and Characterization of Micro and NanoFiber Reinforced Natural Rubber Composites by Latex Stage Processing (Cochin University of Science & Technology, 2012).
18. S. I. A. Razak, W. A. W. A. Wahman, and M. Y. Yahya, *J. Polym. Eng.* **33**, 565 (2013).  
<https://doi.org/10.1515/polvorg-2012-0152>
19. V. P. Anju and S. K. Narayanankutty, *AIP Adv.* **6**, (2016).
20. D. Thanasamy, D. Jesuraj, S. Kumar, and V. Avadhanam, *Polymer* **175**, 32 (2019).  
<https://doi.org/10.1016/j.polymer.2019.03.042>
21. B. Senthilkumar, P. Thenamirtham, and R. K. Selvan, *Appl. Surf. Sci.* **257**, 9063 (2011).  
<https://doi.org/10.1016/j.apsusc.2011.05.100>
22. S. Geetha and D. C. Trivedi, *Synth. Met.* **155**, 232 (2005).  
<https://doi.org/10.1016/j.synthmet.2005.08.003>
23. H. G. B. Premalal, H. Ismail, and A. Baharin, *Polym. Test.* **21**, 833 (2002).  
[https://doi.org/10.1016/S0142-9418\(02\)00018-1](https://doi.org/10.1016/S0142-9418(02)00018-1)
24. A. Pang and H. Ismail, *J. Thermoplast. Compos. Mater.* **27**, 1607 (2014).
25. S. S. Jeon, S. J. Yang, K. -J. Lee and S. S. Im, *Polymer* **51**, 4069 (2010).  
<https://doi.org/10.1016/j.polymer.2010.07.013>
26. R. V. Silva, E. M. F. Aquino, L. P. S. Rodrigues and A. R. F. Barros, *J. Reinf. Plast. Compos.* **28**, 1857 (2009). <https://doi.org/10.1177/0731684408090373>
27. W. Jiao, W. Liu, F. Yang, L. Jiang, W. Jiao, and R. Wang, *Appl. Surf. Sci.* **454**, 74 (2018).  
<https://doi.org/10.1016/j.apsusc.2018.05.145>